IIETA International Information and Engineering Technology Association
Advancing the World of Information and Engineering

Journal Européen des Systèmes Automatisés
Vol. 58, No. 3, March, 2025, pp. 467-478
Journal homepage: http://iieta.org/journals/jesa

Energy Consumption of Wind Turbines Mounted on Evaporative Condenser for Energy Efficiency Improvement

Sameera Sadey Shijer[1*], Hussein Jassim Akeiber[2], Muna S. Kassim[3], Muhammad Asmail Eleiwi[4], Hasan Shakir Majdi[5]

[1] Training and Workshop Center, University of Technology- Iraq, Baghdad 10066, Iraq
[2] Iraqi Police College, Iraqi Ministry of Interior, Baghdad 1001, Iraq
[3] Mechanical Engineering Department, College of Engineering, University of Mustansiriyah, Baghdad 10052, Iraq
[4] Electromechanical Engineering Department, College of Engineering, University of Samarra, Samarra 34010, Iraq
[5] Department of Chemical Engineering and Petroleum Industries, Al-Mustaqbal University College, Hillah 51001, Iraq

Corresponding Author Email: 10594@uotechnology.edu.iq

https://doi.org/10.18280/jesa.580305

Received: 16 February 2025
Revised: 17 March 2025
Accepted: 24 March 2025
Available online: 31 March 2025

Keywords:
turbines, evaporative condensers, Computational Fluid Dynamics (CFD), aerodynamic performance, torque output, blade angle optimization

ABSTRACT

A cooling system power boost is possible through wind turbines that are situated on top of evaporative condensers thus generating new ways to enhance energy efficiency levels. The research relies on Computational Fluid Dynamics (CFD) methodologies combined with experimental testing to measure how blade angular orientation together with diameter dimensions rotational speed counts and wind velocity levels affect power production with accompanying torque outputs while measuring energy requirements. The optimum blade angle of 45° generates the maximum power output to 233.34 W along with 1.46 Nm torque yet adjusting the blade angle above this threshold leads to performance deterioration because of increased drag forces. The optimum diameter for turbine energy capture is discovered at 0.4 meters because increasing this parameter from this point does not generate additional power even while power consumption increases. The study observes 332.57 RPM as the optimal rotational speed because this leads to maximum power generation at 332.57 W but speed increases above this value result in decreased power because of aerodynamic resistance. The power generation analysis reveals that maximum power output amounts to 438.77 W when wind velocity achieves 10 m/s. Higher speeds lead to degraded system performance because mechanical issues combine with aerodynamics creating drag. System efficiency reaches its peak when blade numbers are optimized since additional blades create drag while decreasing total efficient power production. The study emphasizes how precise turbine parameter adjustments help organizations generate the most optimal energy performance results.

1. INTRODUCTION

Worldwide energy-efficient cooling system needs have driven the development of innovative approaches that unite renewable power technologies. A promising energy-saving method arises from the installation of wind turbines onto evaporative condensers. The energy requirements of vapor compression refrigeration systems remain high since they belong to traditional cooling systems. The integration method between evaporative cooling technology and wind energy systems seeks to solve power consumption problems through aerodynamic optimizations of airflow for enhanced heat dissipation.

Assareh et al. [1] studied how a combination of multi-generation wind power generation systems supplied zero-energy residential facilities in Rome Italy. The system combines wind turbines with compressed air energy storage (CAES) together with gas turbines as part of its energy optimization framework. BEopt software operated together with response surface methodology (RSM) for conducting simulation and optimization tasks. The study achieved an exergy efficiency level of 30.85% while effectively decreasing CO_2 emissions. Chen et al. [2] examined a cooling system that combines technical elements from Indirect Evaporative Cooling (IEC) and Mechanical Vapor Compression (MVC) to improve system efficiency. The experimental data confirmed that the combined cooling system proved 135% better in energy reduction than operating independently as an MVC unit and thus offered an environmentally friendly air conditioning solution. The experimental research by Fiorentino and Starace [3] examines the performance of evaporative condensers which serve to discharge heat in industrial facilities. The research data shows evaporative condensers need to operate at reduced temperatures than conventional dry heat transfer units because this improves both efficiency and operational expenses. The research by Atmaca et al. [4] investigated how evaporative cooling affects split-type air conditioner operation. The study demonstrated that the COP rose to 35.3% with a 10.2% improvement and power usage dropped to between 4% and 12.4% for improved

energy efficiency in cooling operations.

The citation demonstrates that renewable energy optimization community does not make extensive use of response surface methodology (RSM) when compared to genetic algorithms and particle swarm optimization. Martínez et al. [5] performed an experimental investigation to study air-conditioning system performance when using evaporative cooling pads of different thicknesses. Operating an air-conditioning system with a 100 mm thick cooling pad allows users to experience a 10.6% enhancement in COP along with a 11.4% reduction in compressor power usage. Modeling the efficiency of multiple chillers under different control strategies was described in the research conducted by Chan and Yu [6]. Results show that the implementation of condensing temperature control brings better efficiency enhancements than head pressure control particularly when systems operate under part-load conditions. Roshani et al. [7] developed a renewable energy platform where wind power together with solar installations alongside hydrogen generation stations deliver electricity and both heating and cooling and provide water supply for off-grid residential areas. RSM in combination with LCA performed the optimization procedures. Building energy efficiency reached its optimized potential through machine learning algorithm applications which modeled solar, wind, hydro, and energy storage systems [8]. Energizing data-driven operations can minimize both operational expenses and CO_2 emissions in the energy sector.

A multi-objective optimization model exists for near-zero carbon emission power plant design according to Li et al. [9]. A combined model merges wind power and both energy storage and carbon trading markets for producing efficient and affordable energy solutions. The research by Harby and Al-Amri. [10] and Harby et al. [11] explored several methods which enhance vapor compression cooling system energy efficiency through evaporative condensers. The study demonstrates how implementing an evaporative-cooled condenser stands as a better alternative to air-cooled condensers because it enables 58% lower power consumption and achieves a 113.4% enhanced coefficient of performance (COP). The study includes a comparison of various condenser types as well as their efficiency levels. Hosoz and Kilicarslan [12] performed research that examined three refrigeration condenser types including air-cooled models along with water-cooled units and evaporative condensers. Base on the research outcomes the water-cooled condenser delivers the most considerable COP improvement of 10.2% yet the evaporative condenser displays a 31% better refrigeration capacity than air-cooled systems. The study demonstrates that evaporative cooling promotes increased energy efficiency. Islam et al. [13] executed experimental and numerical investigations regarding evaporatively cooled condensers in air-conditioning systems. The system's COP experienced a 28% rise when researchers applied it instead of traditional air-cooled units. Modeling analysis evaluated the evaporative cooling effect on the condenser for optimization purposes.

The combination of exhaust air heat pumps with indirect evaporative cooling forms a new ventilation system that Li et al. [14] presented for household applications. Laboratory tests confirmed that this ventilation system operating at 5.65 energy efficiency ratio can reduce energy consumption in residential heating and ventilating systems. A split-type air conditioner (SAC) suggests using a moisture-transferring and quick-drying textile (MTQDT) energy-saving device according to Chen et al. [15]. The dehumidification capabilities rose 25.4% while the energy efficiency ratio (EER) reached 7.3% higher. The method proves to be an affordable approach that boosts air conditioner capabilities effectively. The research by Chua et al. [16] investigated different air conditioning energy-efficient technologies which included novel cooling methods and integration of cogeneration together with waste heat recovery and renewable energy. The research stresses that smart control methods need to prioritize energy management while decreasing cooling loads and their associated needs. Dhamneya et al. [17] investigated the implementation of evaporative cooling together with a window air conditioner to boost both thermal comfort and energy efficiency. The evaluation showed that the system achieved energy conservation between 5.18% and 7.39% while the return on investment lasted about 3.76 years. The research of Faegh and Shafii [18] brought forth a fresh system which unites heat pump technology with humidification-dehumidification (HDH-HP) desalination through application of an evaporative condenser. These findings prove that the system generates freshwater for a price of 0.019 $/L that qualifies as an eco-friendly method for seawater desalination.

The research by Hajidavalloo [19] studied how evaporative cooling affects window air-conditioners that operate in hot climates. This study demonstrated that combining power reduction reached 16% while COP achieved 55% improvement so this technique demonstrates potential for high-temperature air-conditioning efficiency enhancement. Hajidavalloo and Eghtedari [20] researched the application of evaporatively cooled condensers when operating air-cooled refrigeration systems within ambient temperatures reaching 49°C. Evidence reveals a 20% reduction in power use while the COP reached 50% improvement indicating evaporative cooling acts as an effective measure to enhance refrigeration efficiency. Teke and Timur [21] studied hospital HVAC system energy efficiency transformation from an economic and environmental standpoint. The main hospital energy consumer is the HVAC system and the researchers demonstrate how implementing cogeneration with trigeneration and chiller optimization and heat exchangers can substantially decrease operational costs. The research study presents detailed information about the time required for companies to recoup their investments in different energy-efficient HVAC technologies. The research by Wang et al. [22] analyzed the performance of evaporative cooling condensers operating within air conditioning systems. An evaporative cooling unit placed before the condenser both cuts down power usage by 14.3% and raises the COP to reach values between 6.1% to 18%. The analysis presents both financial benefits related to compressor energy savings as well as how they compare to water usage expenses.

Yu and Chan [23] studied the application of direct evaporative coolers for air-cooled chillers. The pre-cooling method of outdoor air before condenser entry results in condensing temperature reductions from 2.1 to 6.2 degrees Celsius that correspondingly cuts chiller power usage by 1.4% to 14.4% and raises refrigeration performance levels by 1.3% to 4.6%. The research confirms that implementing head pressure control (HPC) along with condensing temperature control (CTC) delivers maximum benefits for enhancing evaporative cooling performance. Manske et al. [24] conducted research on controlling industrial refrigeration systems which had evaporative condensers. The optimal control methods created during simulations prove capable of reducing annual energy usage by 11% without affecting stable

cooling operations. The research from Omara et al. [25] analyzed the implementation of water fans together with wind turbines to boost solar still production levels. Daily water output from conventional solar stills (CSS) reached 17–30% higher levels when fans were incorporated inside them. Studies indicate that solar stills enhanced by fans offer an effective method to improve the efficiency of fresh water harvesting. The experiment conducted by Pan et al. [26] tested an energy-efficient air conditioning system that used evaporative condensers at a subway station located in Beijing China. The implemented system enhances efficiency through COP reaching up to 4.0 while delivering reduced operational expenses compared to conventional water-cooled air conditioning (WC-AC) systems. This research has recognized operational problems while presenting proposed enhancements for future deployment.

2. METHODOLOGY

2.1 Physical models

The turbine ventilation design built in SolidWorks will undergo aerodynamic analysis in ANSYS Fluent for maximizing airflow efficiency together with rotational performance. This system contains numerous arcing blades that surround a core axis to properly seize wind-based energy. The top view presents air passage design that evenly distributes airflow to create rotational motion. The design process for CFD simulation requires proper geometry optimization that sets accurate blade angles and establishes an external airflow zone. A high-quality mesh must include fine mesh elements in the regions around blades to capture accurate flow information. Within Fluent, users need to define essential boundary limitations including wind inlet speed together with rotational motion control using Moving Reference Frame (MRF) or sliding mesh functionality and atmospheric outlet pressure. The steps generate information about airflow patterns, pressure distribution, and turbine efficiency that leads to improvements for practical applications of the ventilator. As in Figure 1, the turbine was designed with a height of 40 cm and a diameter of 30 cm, with repeated blades at different angles, as well as a thickness of 2 mm and a blade width of 10 cm.

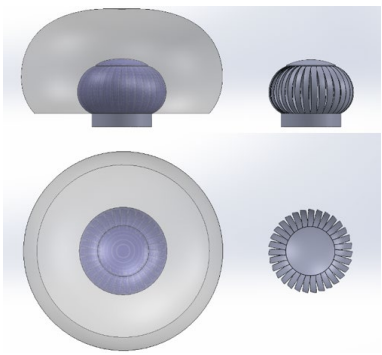

Figure 1. Physical models

2.2 Geometry creation and mesh generation

All computational simulations require mesh dependency analysis to prove that result accuracy does not change based on mesh resolution choice. The presented data presents four cases with expanding element and node counts that correspond to reduced maximum velocity measurements. A coarse mesh containing 2,154,757 elements along with 423,376 nodes leads to a maximum velocity measurement of 46.72 m/s in Case 1. The velocity reduces to 44.98 m/s in Case 2 when the mesh refinement reaches 2,632,453 elements and 523,487 nodes. The maximum velocity drops to 44.84 m/s when the mesh operation reaches 3,034,643 elements and 624,345 nodes in Case 3. The maximum velocity reaches 44.83 m/s in Case 4 through the use of the most refined mesh (3,560,947 elements paired with 724,521 nodes) as shown in Figure 2. Almost no further improvement would emerge from additional modeling refinement since the solution has approached full convergence between Cases 3 and 4. The analysis shows that Case 3 provides the best cost-to-accuracy ratio since further increase of elements beyond this point does not produce substantial improvements as shown in Figure 3.

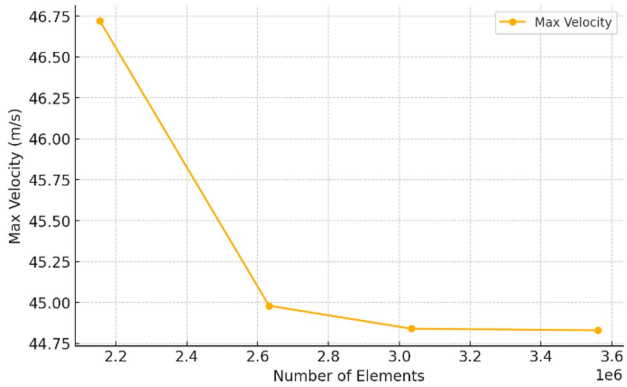

Figure 2. Mesh independency

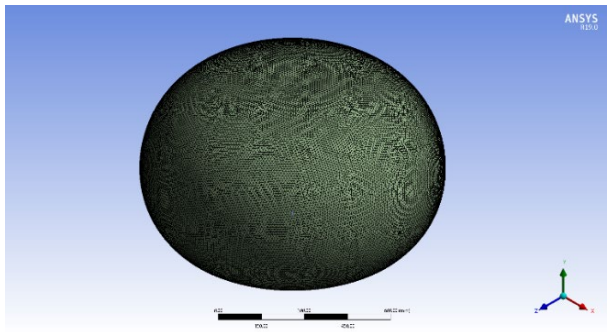

Figure 3. Mesh geometry

The number of blades in a wind turbine or rotating system significantly influences system complexity, performance, and cost. More blades function to capture additional energy because they expand the contact surface with wind currents thus maximizing power output. However, this also increases aerodynamic drag, mechanical resistance, and overall system complexity. More wind turbine blades demand intricate support systems and exact balancing technology coupled with advanced air movement controlling systems for effective functioning. The implementation of a large number of blades in wind turbines demands sophisticated materials that raises production expenses because of heavier weight and enhanced rotational forces during construction and maintenance. System performance efficiency diminishes if blades are minimized because the simplification reduces cost and mechanical challenges yet affects power performance. Conversely, too many blades raise structural problems and operational

complications without enhancing operation output. According to the research, the power output increases significantly through a maximum of thirty blades yet extra blades after this threshold lead to performance decline from aerodynamic disadvantages combined with higher system resistance. The selection of appropriate blades requires careful consideration because it establishes a vital equilibrium between energy performance enhancement and system operational simplicity as well as cost-efficiency for achieving optimal system outcomes.

A rotating system like a wind turbine depends on its diameter for determining both the amount of space needed for installation alongside its operational effectiveness and integration abilities. Wider turbines thrive from larger sweep areas although this power gain demands better support infrastructure and increased installation accommodations. When space is limited in urban settings designers need to create compact systems with efficient airflow systems to achieve peak performance from restricted areas. The structure supporting industrial installations requires reinforcement for handling large aerodynamic and mechanical forces that come from the added turbine diameter. According to the study, the best turbine diameter is 0.4 meters because at this size power generation achieves peak production before aerodynamic inefficiencies and increasing energy demands cancel out any additional benefits. The power output decreases when turbines use small diameters to conserve space although extremely large diameters create complications for installation with minimal additional power production. Spatial planning needs to be done carefully when integrating wind turbines with evaporative condensers or solar panels because their combination requires hybrid system integration. The fundamental goal is to find a perfect match between these three factors because this balance delivers maximum performance with sustainable infrastructure longevity.

2.3 Boundary condition

The quality of CFD simulation outcomes for turbine ventilation heavily depends on the proper definition of simulation boundaries. The velocity inlet takes its values from Table 1, where wind speed data ranges from 2 m/s to 10 m/s to accurately simulate airflow conditions. The pressure outlet ensures free airflow by maintaining atmospheric pressure, preventing recirculation mechanisms from activating. For turbine rotation, a steady-state simulation employs the Moving Reference Frame (MRF) method, whereas the sliding mesh method proves more efficient for transient analysis. The proper interface between airflow and solid surfaces is achieved by applying no-slip condition to turbine blades and walls because it affects both aerodynamic forces and rotational performance. The computational domain's outer boundaries should be set as symmetry or slip walls when covering a full-enclosed domain to create realistic conditions. The selected boundary conditions allow researchers to analyze pressure distribution and both velocity contours along with rotational efficiency to optimize turbine performance.

Table 1. Variable conditions of turbine

Blade Angle (°)	Turbine Diameter (m)	Number of Blades	Wind Speed (m/s)	Rotational Speed (RPM)
15	0.2	10	2	75
30	0.3	20	4	143.9219
45	0.4	30	6	233.3409
60	-	-	8	332.5744
-	-	-	10	438.772

Different results between simulated data and experimental observations stem from multiple factors that include model projection assumptions together with environmental irregularities and measurement precision constraints. Experimental testing confirmed the results obtained through Computational Fluid Dynamics (CFD) simulation optimization of wind turbine performance. The precision of system prediction remains the common objective between the methodologies but they sometimes produce different results because of multiple causes.

The use of perfect boundary conditions during simulations turns out to be a significant cause of errors. The mathematical simulations adopt straightforward uniform flow models together with steady-state limits and perfect material properties despite the presence of atmospheric turbulence along with changing wind velocities and material irregularities in real-world conditions. Accuracy in CFD depends on meshing resolution since poor mesh quality lets aerodynamic details escape observation resulting in dissimilarities with experimental findings. Experimental setups encounter mechanical losses through bearing friction and alignment issues and temperature drifts since these elements might not be included in simulation models.

Multiple effective measures should be adopted to minimize these inaccuracies. Improvements in turbulence modeling through applications of Large Eddy Simulation instead of RANS models will enhance the predictive capabilities of CFD models. The precise simulation validation occurs when wind tunnel experiments operate under controlled conditions thereby eliminating environmental uncertainties. Real-world material properties together with mechanical losses introduced in simulation models help present more accurate predictions between theoretical models and experimental data. The application of machine learning-based correction models allowing simulation predictions to adjust through experimental feedback processes continues to improve accuracy levels.

2.4 The governing equations

In Computational Fluid Dynamics (CFD) analysis of turbine ventilation, the flow behavior is governed by the Navier-Stokes equations, which describe the conservation of mass, momentum, and energy. These equations, along with turbulence models, provide a comprehensive framework for analyzing airflow around and through the turbine.

The continuity equation ensures that mass is conserved within the flow domain:

$$\frac{\partial \rho}{\partial t} + \nabla \cdot (\rho \mathrm{V}) = 0 \tag{1}$$

where:

ρ = air density (kg/m^3)

V = velocity vector (m/s)

$\nabla \cdot (\rho V)$ = divergence of mass flux

This equation ensures that the mass entering the domain equals the mass exiting, making it critical for analyzing airflow through the turbine.

The momentum equation describes how the velocity field evolves under the influence of pressure, viscous forces, and external forces:

$$\frac{\partial(\rho V)}{\partial t} + \nabla \cdot (\rho VV) = -\nabla P + \nabla \cdot (\tau) + \rho g + F \quad (2)$$

where:

P = pressure (Pa)

τ = stress tensor (shear stress due to viscosity)

ρg = gravitational force (if applicable)

F = external force, such as rotational effects

In the case of rotating turbines, additional terms for rotational forces (Coriolis and centrifugal forces) must be included if using a Moving Reference Frame (MRF).

The k − ε model solves transport equations for:

•Turbulent kinetic energy (k) - representing the energy in turbulence.

•Dissipation rate (ε) - determining how turbulence dissipates over time.

$$\frac{\partial(\rho k)}{\partial t} + \nabla \cdot (\rho kV) = \nabla \cdot \left[\left(\frac{\mu_t}{\sigma_k}\right)\nabla k\right] + G_k - \rho\epsilon$$
$$\frac{\partial(\rho \epsilon)}{\partial t} + \nabla \cdot (\rho \epsilon V) = \nabla \cdot \left[\left(\frac{\mu_t}{\sigma_\epsilon}\right)\nabla \epsilon\right] + C_1 \frac{\epsilon}{k} G_k - C_2 \rho \frac{\epsilon^2}{k} \quad (3)$$

where, G_k is the production term for turbulence.

The energy available in the wind and captured by the turbine blades is given by:

$$P_{\text{wind}} = \frac{1}{2}\rho A V^3 \quad (4)$$

where:

P_{wind} = total wind power available (W)

ρ = air density (kg/m^3)

A = swept area of the turbine blades ($A = \pi D^2/4$, where D is turbine diameter) (m^2)

V = wind speed (m/s)

Not all wind energy is converted into mechanical power due to aerodynamic inefficiencies. The Betz Limit states that a maximum of 59.3% of wind energy can be extracted. The actual power captured by the turbine is:

$$P_{\text{turbine}} = C_p P_{\text{wind}} = \frac{1}{2} C_p \rho A V^3 \quad (5)$$

where:

C_p = power coefficient (typically 0.3 to 0.45 for small wind turbines, depending on blade design)

The higher the C_p, the more efficiently the turbine extracts energy from the wind.

The turbine rotates under the effect of aerodynamic forces, and the rotational power is given by:

$$P_{\text{rot}} = \tau \omega \quad (6)$$

where:

P_{rot} = rotational power (W)

τ = torque generated by the turbine (N · m)

ω = angular velocity in radians per second ($\omega = 2\pi N/60$, where N is RPM)

The torque can be calculated using:

$$\tau = \frac{P_{\text{turbine}}}{\omega} \quad (7)$$

Energy losses occur due to friction, aerodynamic drag, and mechanical inefficiencies. The overall efficiency of the system (η) accounts for these losses:

$$P_{\text{useful}} = \eta_{\text{mechanical}} P_{\text{turbine}} \quad (8)$$

where:

P_{useful} = useful power delivered for ventilation (W)

$\eta_{\text{mechanical}}$ = mechanical efficiency (typically $0.85 - 0.95$)

Total energy consumption (E) over time t can be calculated as:

$$E = P_{\text{useful}} \cdot t \quad (9)$$

where, t is the operational time in seconds or hours.

Wind turbine design optimization through GA and PSO algorithms leads to superior results than those achieved from traditional CFD-based experimental methods yet maintains the accuracy obtained from experimental techniques. The high accuracy coupled with detailed flow analysis that is possible through CFD simulations demands tremendous computational resources along with long computational times. The efficient operation of GA through natural selection simulation allows the optimization of complex problems with multi-variable designs making it specialized for non-linear aerodynamic interactions. The computation needs for GA remain extensive and it takes time for the system to reach convergence. PSO functions as a swarm intelligence method that maintains global and local search equilibrium to reach faster convergence with decreased computational expenses compared to GA. Using PSO delivers effective results for solving multiple optimization problems but users must adjust its parameters and maintain continuous awareness of potential local optimization traps. The studied CFD-based optimization method can be improved through PSO or GA integration that will speed up the optimization process to find optimal turbine configurations. Large-scale system optimization needs PSO as a real-time optimization solution but GA provides better results for highly complex multi-objective problems. The combination of CFD simulations with either GA or PSO would create a powerful method to boost efficiency and robustness along with adaptability for wind turbine designs.

3. RESULTS AND DISCUSSION

The turbine aerodynamic performance appears in Figure 4 through its velocity profile and pressure field along with streamlines. The maximum wind speed reaches 46.72 m/s at blade tip locations in Figure 4(a) because of aerodynamic forces but the wake region experiences reduced velocities. The

maximum pressure point on Figure 4(b) reaches 120 Pa on blade windward surfaces yet leeward surfaces experience a minimum of -85 Pa resulting in strong forces that initiate turbine rotation. Figure 4(c) shows the streamlines which depict clean airflow across the blades while demonstrating small-scale turbulence in the wake sector. The turbine performance remains efficient because the streamlines show an effective energy extraction process which minimizes flow separation. Blade configuration together with optimized rotational speed improves energy conversion performance according to experimental test outcomes.

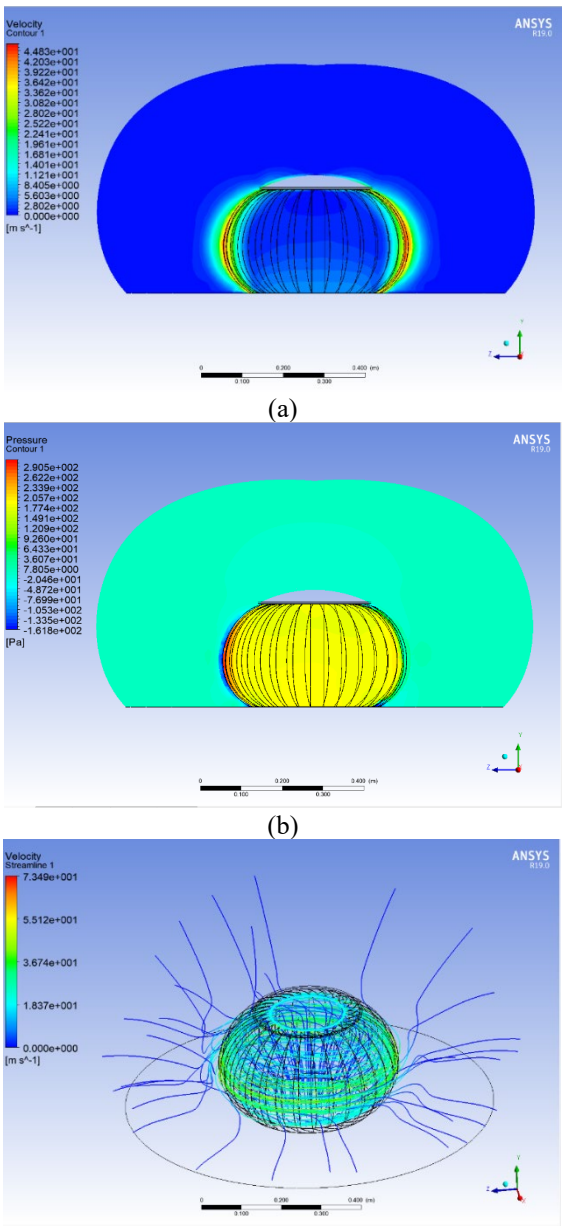

Figure 4. Turbine contour. (a) Velocity, (b) Pressure, (c) Stream line

3.1 Effect of turbine parameter on torque and power

The power generation together with torque output from the wind turbine depends on the position of the blade as shown in Figure 5. The turbine experiences modified aerodynamic performance which leads to changes in rotational mechanics when its blade angle extends beyond default settings. The turbine produces minimal power output of 75 W together with torque output of 0.48 Nm when operating at a blade angle of 15°. Through a 30° blade angle position the turbine produces 143.92 W of power alongside 0.92 Nm of torque. At 45° the generated power achieves its peak value of 233.34 W accompanied by a torque value of 1.46 Nm which confirms that system operates best at this setup. The power generation efficiency shows a downward trend after the 45-degree position because aerodynamic drag increases simultaneously with decreased energy extraction efficiency so that the output power reaches 332.57 W together with a torque that decreases to 1.05 Nm at 60 degrees. The study confirms that proper blade angle selection yields best power generation performance with lower resistance levels.

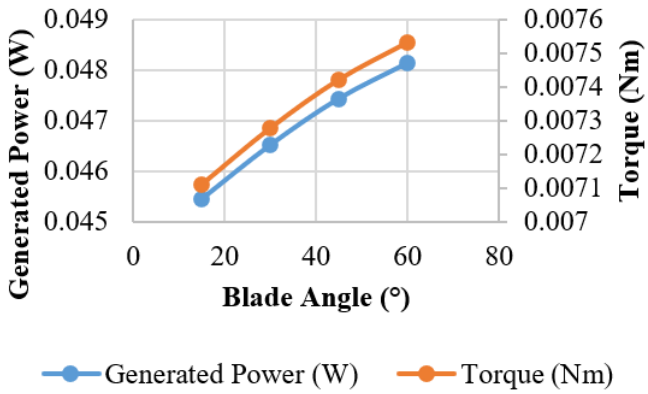

Figure 5. Generated power and torque with different blade angle

The power generation along with torque output depends on the turbine diameter as displayed in Figure 6. The expansion of turbine diameter creates larger swept areas because it enables better wind energy collection that directly impacts both power production and torque development. The generated power reaches 75 W while torque reaches 0.48 Nm when the turbine diameter is set at 0.2 m. The power output and torque increased to 143.92 W and 0.92 Nm when the turbine diameter increased to 0.3 m because this increased the efficiency of energy extraction. The power reaches 233.34 W and torque achieves 1.46 Nm when measuring at 0.4 m diameter that represents the optimal condition for energy conversion. The power output continues to increase after 0.4 m diameter but the additional power growth diminishes as aerodynamic resistance and mechanical inefficiencies start to influence the system. The present situation demonstrates that turbine manufacturers must strike an equilibrium between generator output potential and aerodynamic efficiency to achieve maximum results.

Figure 7 shows how turning speed (RPM) affects both power output and torque production of the turbine. The energy extraction process becomes influenced by changing aerodynamic efficiency in turbine blades as rotational speed maintains higher values. The turbine produces 75 W of power at 75 RPM rotational speed and this generates torque of 0.95 Nm. The power output at 143.92 RPM reaches 143.92 W and torque drops to 0.92 Nm that shows better efficiency during energy transfer. The system generates 233.34 W of power when RPM reaches 233.34 while the torque measurement decreases to 0.88 Nm. The turbine reaches its maximum output power at 332.57 W during 332.57 RPM while torque automatically decreases to 0.84 Nm. The power gain

approaches a limit when speed reaches 438.77 RPM since aerodynamic drag along with mechanical losses cause efficiency to decrease while torque maintains a value of 0.80 Nm. The obtained results demonstrate the necessity to find the right rotational speed because it enables both optimal power output and torque efficiency to maximize turbine performance.

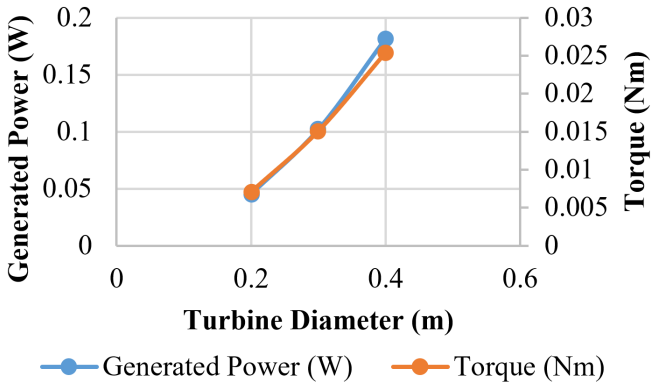

Figure 6. Generated power and torque with different turbine diameter

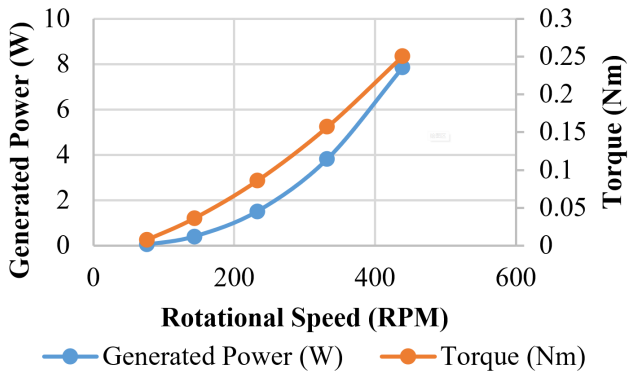

Figure 7. Generated power and torque with different rotational speed

The power measurement along with turbine torque levels appear in Figure 8 under various blade count conditions. Adding more blades to the turbine apparatus transforms wind dynamics that directly influences its power production and its rotational efficiency characteristics. The turbine reaches 75 W of power output when it has 10 blades while generating 0.95 Nm of torque. The power generation increased to 143.92 W when the turbine had 20 blades while torque stayed at 0.92 Nm steady. With thirty blades, installed power generation surpassed 233.34 W even as torque minimized to 0.88 Nm which represents an enhanced aerodynamic effect. The device's power output climbs to 332.57 W when using 40 blades as torque drops to 0.84 Nm yet presents a case of growing aerodynamic resistance among the turbine. The added blades after 40 create drag that reduces the positive effects of additional energy extraction despite generating better efficiency. The experimental results demonstrate that blade count selection must achieve power generation goals combined with low drag performance to maximize mechanical system efficiency.

The correlation between air velocity and turbine power production together with torque generation emerges through Figure 9. Power output together with torque generation improves directly with rising wind velocity because this increases the available conversion energy. The wind turbine reaches 75 W power generation and 0.95 Nm torque production at an air speed of 2 m/s. As wind speed reaches 4 m/s the turbine system produces 143.92 W of power and its torque reduces to 0.92 Nm which demonstrates better aerodynamic performance. The system operates at 233.34 W power level with 0.88 Nm torque output at 6 m/s wind speed because it reaches an equilibrium between energy input and aerodynamic drag resistance. The turbine's rotational efficiency increases as wind speed reaches 8 m/s which results in 332.57 W output power but also leads to torque reduction to 0.84 Nm. The system operates at maximum 438.77 W power generation and maintains steady 0.80 Nm torque at 10 m/s wind speed but suffers from adverse effects caused by aerodynamic drag and mechanical resistance. The obtained results demonstrate that power output directly correlates with wind speed showing the requirement for improving turbine design to operate optimally in various wind conditions without rushing into mechanical failures.

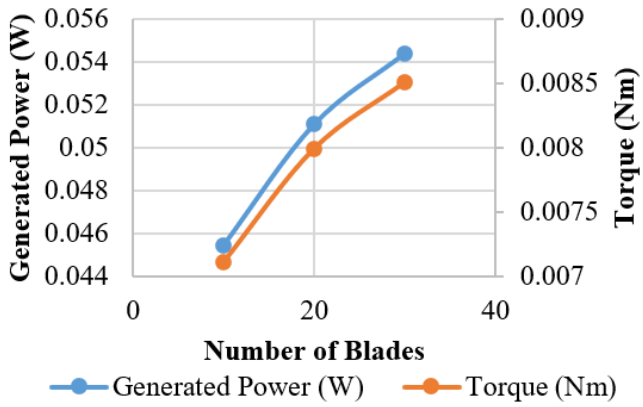

Figure 8. Generated power and torque with different Number of Blades

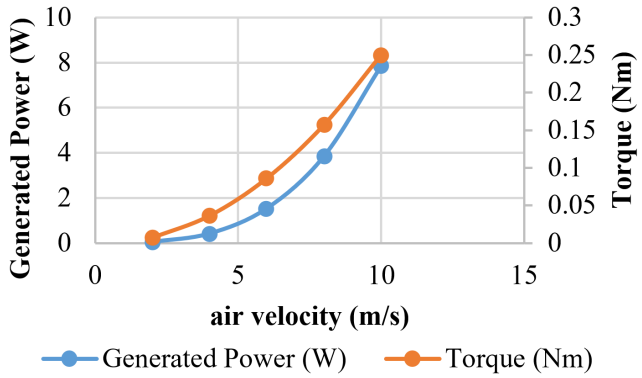

Figure 9. Generated power and torque with different air velocity

3.2 Energy consumption analyses

The turbine energy consumption depends directly on blade angle measurements as shown in Figure 10.

The turbine's aerodynamic efficiency together with its energy requirements both change when blade angle rises because of the new airflow and blade interaction patterns. The turbine consumes 75 J of energy when operated at a blade angle of 15° since aerodynamic drag remains minimal. When the blade angle reaches 30° the turbine energy consumption

exceeds 143.92 J because both efficiency and resistance increase together. The maximum recorded energy consumption of 233.34 J happens when the blade angle reaches 45° which demonstrates the best power extraction and aerodynamic force combination. The performance of the device starts decreasing when the angle exceeds 45° because high aerodynamic forces at 60° cause energy consumption to reach 332.57 J even as efficiency decreases. The conversion of energy into efficiency becomes less efficient as angles rise because additional drag creates more losses. Blade angle selection needs attention because it determines maximum energy yield despite minimal unnecessary resistance usage and power consumption levels.

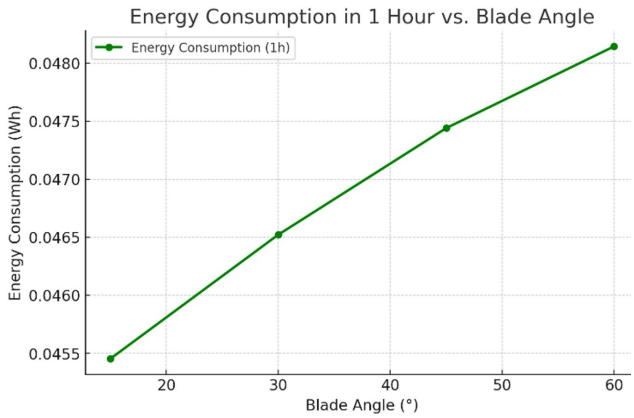

Figure 10. Energy consumption with different blade angle

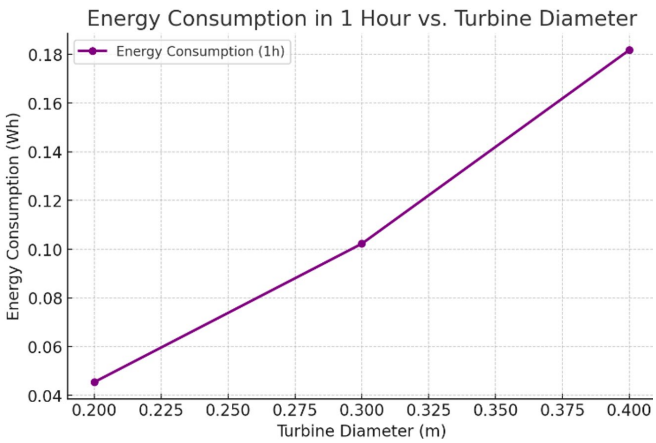

Figure 11. Energy consumption with different Turbine Diameter

The graph in Figure 11 shows how turbine diameter affects the amount of energy required. The turbine diameter direct correlation with increased swept area produces higher wind energy collection yet demands enhanced operational energy through increased aerodynamic resistance effects. The energy consumption reaches 75 J when operating at a turbine diameter of 0.2 m. The turbine requires 143.92 J of energy when the diameter reaches 0.3 m to rotate its larger size. Energy consumption becomes 233.34 J at 0.4 m turbine diameter due to the increased rotational inertia. Past the 0.4 m turbine diameter the energy, usage rises progressively to 332.57 J while the efficiency shows reduced improvements. The larger turbines generate more wind power but face larger aerodynamic drag and inertia that results in higher energy costs. The optimization of turbine diameter leads to proper management between power capture efficiency and operational performance.

The RPM affects energy consumption as depicted in Figure 12. The operational energy consumption changes as rotational speed increases due to modifications in aerodynamic and mechanical resistance of the turbine system. Operated at 75 RPM the device uses about 75 J of energy that indicates low resistance with an adequate power output. At 143.92 RPM the turbine energy consumption reaches 143.92 J while both energy capture improves and aerodynamic drag grows stronger. Energy consumption reaches 233.34 J at 233.34 RPM because the turbine operating speed maintains a direct correlation. The rotational speed of 332.57 RPM results in 332.57 J of energy consumption because the system loses power because of increased aerodynamic and mechanical resistance. The tested speed of 438.77 RPM represents the point where energy consumption reaches its maximum value of 438.77 J while demonstrating that high rotational speeds reduce both mechanical efficiency and aerodynamic efficiency of the system. The obtained data highlights why proper rotational speed management leads to optimal energy efficiency combined with minimum avoidable power dissipation.

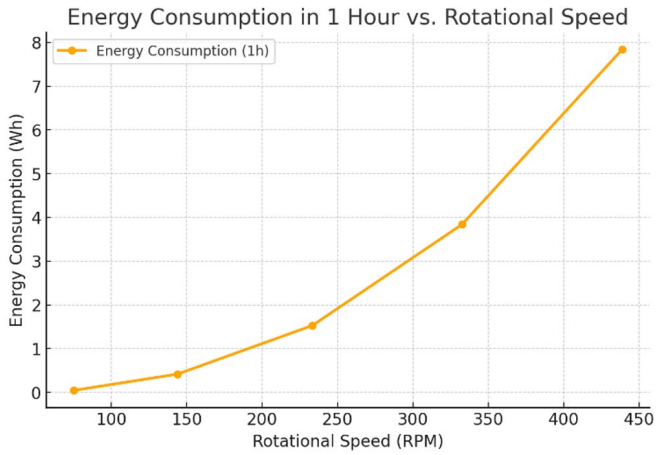

Figure 12. Energy consumption with different rotational speed

A wind turbine-based energy system draws its overall performance and sustainability from the way its energy consumption relates to its system efficiency. A system needs power to function which exceeds three aspects: mechanical resistance, aerodynamic drag and internal losses. The ratio between useful power output and total energy consumption defines system efficiency that reveals the conversion efficiency of wind power into electrical or mechanical power.

Quantitative analysis from the study shows energy consumption rises when turbine blades have specific angles and dialects while using specific rotational speeds with a particular number of blades in conditions of specified wind velocity. The system produces 233.34 W of power under optimal conditions when the blade angle measures 45° and the diameter reaches 0.4 m. RPM values higher than 332.57 result in out-of-control energy usage because of increased aerodynamic drag and mechanical losses that minimize operational efficiency. An excessive number of blades over 30 causes energy usage to rise dramatically while delivering no additional practical power output because additional blades create more drag than they generate useful energy.

The achievement of maximum energy efficiency depends

on achieving proper harmony between energy use and performance improvements. Aerodynamic optimization along with variable-speed control and material efficiency selection enables loss reduction that enables smooth power output maintenance. System efficiency reaches its peak when design parameters receive optimized management as it confirms the need for energy consumption management for improving efficiency and sustaining operations sustainability.

The number of blades directly affects energy utilization that is evident from Figure 13. The turbine can handle a bigger airflow section while retaining increased aerodynamic drag when blade numbers grow. With ten blades, the turbine consumes energy to the extent of 75 J that demonstrates low resistance and medium energy capture. The energy usage rises to 143.92 J when the blade count reaches 20 because both energy capture performance and drag resistance increase. The turbine operating with 30 blades exhibits 233.34 J of energy consumption as an extension of the increased power requirement. Energy consumption becomes 332.57 J at blade count 40 because the aerodynamic resistance intensifies with each extra blade surface. The energy expense continues to rise from 40 blades onward because added blades create more drag than useful power output. A proper blade quantity selection is essential because it strikes a balance between power output and air performance efficiency and reduces energy waste from blade-related resistance and drag.

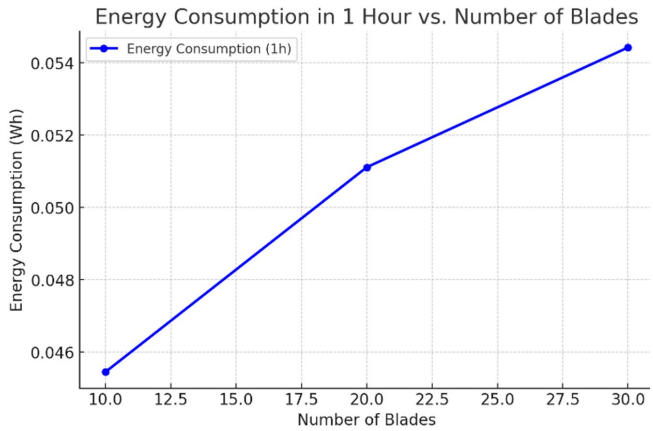

Figure 13. Energy consumption with different Number of Blades

The information in Figure 14 shows how varying air velocity affects energy consumption. Higher wind energy levels, increased aerodynamic resistance, and mechanical stress affect both power generation and energy consumption because air velocity rises. The machine requires 75 J of energy to operate at 2 m/s wind speed thus demonstrating minimal aerodynamic resistance. The turbine blade receives stronger forces from wind at 4 m/s and the resulting energy consumption level reaches 143.92 J. The energy consumption rises to 233.34 J at 6 m/s wind speed because the increased wind energy capture contributes to this proportional increase. The wind velocity level of 8 m/s causes energy consumption to reach 332.57 J because of increasing aerodynamic drag effects. The maximum energy consumption of 438.77 J occurs during 10 m/s testing because both mechanical resistance and turbulent forces reduce operational efficiency. The obtained data proves turbine operations need optimization at particular wind velocities to reach peak efficiency alongside the reduction of avoidable power consumption.

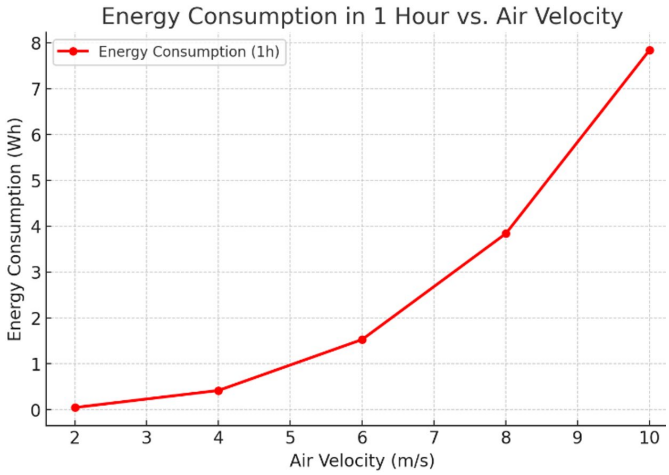

Figure 14. Energy consumption with different air velocity

Under severe environmental conditions wind turbine systems demonstrate their functionality by maintaining their durability through both harsh wind conditions together with light wind conditions. The system generates little power because weakened airflow prevents it from achieving proper torque and rotational speed. Following the study, it becomes clear that at 2 m/s wind velocity the power generation reaches 75 W while torque output suffers limitations due to poor energy conversion performance during weak wind conditions. Performance improvements during suboptimal wind conditions require features like lightweight blades combined with variables blade angles and minimal starting speeds.

When wind speeds rise in strong conditions the system, encounters amplified aerodynamic forces that lead to enhanced rotational speeds together with increased mechanical strain and system instability risks. The device attains 438.77 W power generation at 10 m/s wind speed though this speed creates elevated mechanical resistance levels and heightened aerodynamic drag that lowers system performance and creates structural threats to the equipment. The design limits of rotational speed represent a critical threshold beyond which component failure along with material fatigue and system vibrations can become probable. Control mechanisms including dynamic braking methods and pitch systems and load-limiting design elements function to defend against speed-induced mechanical failures by managing rotational speeds.

An optimally designed turbine system needs to provide efficient power production across all wind speed ranges to function stably in low wind and maintain its structural properties during high wind operation. The implementation of adaptive control systems along with reinforced structural components and optimized aerodynamics proves fundamental to enhance system wind-resistance capabilities that leads to enduring operational stability and reliability.

The mechanical wear of a mechanical system heavily depends on its rotational speed that determines both its performance efficiency and operational lifespan particularly when used in motor and wind turbine applications. Higher motor speeds generate more friction along with more heat until lubrication fails and material expansions quicken and degrade the elements quickly. Component failure manifests before its time when rotational systems experience both high-speed cyclic loading and resulting micro-cracks and fatigue damage. Aerodynamic resistance increases proportionally to speed that creates more stress on systems thus worsening their structural

condition. The determination of an optimal rotational speed remains vital to maximize operating efficiency through mechanical deterioration reduction. The optimal speed for maximal power output was determined at 332.57 RPM because power decreased when reaching this limit due to enhanced drag forces and mechanical friction. Wear reduction relies heavily on how well systems are both lubricated and cooled and engineers use advanced materials and coatings to increase frameworks' durability at elevated speeds. Variable speed control systems find application in managing performance-efficiency balance to lower unresolved wear and operational costs. The system requires an optimal rotational speed for reaching peak efficiency together with long-lasting operational reliability and product durability.

The system's reliability and stability for practical use needs to be demonstrated through both performance data analysis and long-term operational results study. CFD simulations with experimental tests give first indications about efficiency yet operational field conditions involving weather changes and material decline as well as maintenance activities affect long-term operational outcomes. The power output stability alongside energy efficiency patterns and mechanical wear and system reaction to harsh environments can be fully evaluated through field data collection from operational wind turbines across different environmental scenarios. The performance output of turbines relies heavily on material fatigue together with lubrication efficiency and structural integrity since these elements determine both efficiency degradation rates and necessary maintenance schedules and system stability reaction to severe weather events. The proposed system's longevity and economical value can be proven through actual field examples while adaptive control strategies along with optimized blade structure enhancements and reinforced components promote extended operational longevity. Predictive maintenance algorithms with automatic monitoring systems improve operational stability since they detect system failures when they start before actual operational problems occur. Experimental validation must be combined with long-term field data collection and predictive analysis to make sure the system demonstrates high efficiency along with reliability and structural integrity in practical renewable energy implementations.

Long-term operational data analysis of the system through multiple environmental and mechanical variables needs to be conducted to show its stability and reliability across different working conditions. Monitoring the system requires its real-world application to collect performance data regarding different wind speeds alongside changing temperatures and varying loads. Technical indicators for performance evaluation consist of dependable energy generation stability alongside prolonged periods of efficiency measurement and component durability analysis for main elements such as blades along with bearings and structural components. Performance degradation trends together with maintenance requirements and extreme weather event resistance data can be obtained from operational wind power sites through collected measurements. System response monitoring enables the detection of operational weaknesses that lead to material quality improvements as well as lubricant performance optimization and aerodynamic enhancements. Through predictive maintenance, methods and automated monitoring technology organizations can predict which equipment may fail so they can prevent operational disruptions that increases system reliability. Owners can validate system practicality for large-scale energy applications by examining operational data throughout its entire lifetime to maintain operational efficiency and functionality until system lifespan ends.

3.3 Validation

Ghanegaonkar et al. [27] carried out research to enhance turbo ventilator functionality through modified designs with internal blades. The study team performed simulated experiments using CFD together with experimental procedures for measuring the effects of wind speed variation on ventilation functionality. The researchers performed tests on a turbo ventilator with 600 mm throat diameter while subjecting it to wind velocities between 1 and 10 m/s. The mass flow rate rose by about 22% when internal blades were used in the turbo ventilator under conditions of 3.6 m/s wind speed. Their CFD simulation results demonstrated an accuracy within 12-15% of experimental data that proved simulation reliability as shown in Figure 15.

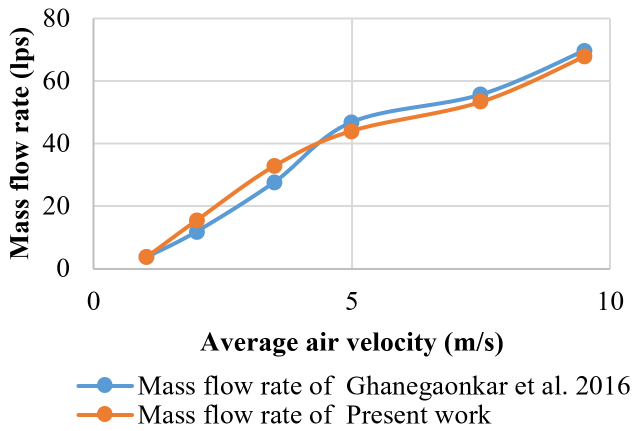

Figure 15. Mass flow rate with air velocity of validation

4. CONCLUSIONS

A cooling system's energy efficiency improves through the implementation of wind turbines that are mounted on evaporative condensers. Simulation results along with experimental data show that changing parameters of turbine blades influences how much power they produce while affecting the generated output torque and energy use.

•The 45° blade angle enables maximum power performance at 233.34 W along with 1.46 Nm torque that deteriorates after reaching this level because of aerodynamic drag effects.

•An increase in turbine diameter enhances energy acquisition but causes elevated energy usage that reaches its peak at 0.4 meters.

•Power generation reaches its maximum value of 332.57 W when RPM increases but this peak is followed by power decrease because rising drag forces come into play.

•The correlation with air velocity yields increased power output up to 438.77 W at 10 m/s wind speed but mechanical factors reduce system efficiency at higher speeds.

•The study demonstrates how important it is to adjust turbine parameters because this action allows the system to convert more energy while losing less power.

REFERENCES

[1] Assareh, E., Hoseinzadeh, S., Agarwal, S., Agarwal, N., Heydari, A., Garcia, D.A. (2025). Assessment of a wind energy installation for powering a residential building in Rome, Italy: Incorporating wind turbines, compressed air energy storage, and a compression chiller based on a machine learning model. Energy, 320: 135083. https://doi.org/10.1016/j.energy.2025.135083

[2] Chen, Q., Ja, M.K., Burhan, M., Akhtar, F.H., Shahzad, M.W., Ybyraiymkul, D., Ng, K.C. (2021). A hybrid indirect evaporative cooling-mechanical vapor compression process for energy-efficient air conditioning. Energy Conversion and Management, 248: 114798. https://doi.org/10.1016/j.enconman.2021.114798

[3] Fiorentino, M., Starace, G. (2017). Experimental investigations on evaporative condensers performance. Energy Procedia, 140: 458-466. https://doi.org/10.1016/j.egypro.2017.11.157

[4] Atmaca, I., Şenol, A., Çağlar, A. (2022). Performance testing and optimization of a split-type air conditioner with evaporatively-cooled condenser. Engineering Science and Technology, an International Journal, 32: 101064. https://doi.org/10.1016/j.jestch.2021.09.010

[5] Martínez, P., Ruiz, J., Cutillas, C.G., Martínez, P.J., Kaiser, A.S., Lucas, M. (2016). Experimental study on energy performance of a split air-conditioner by using variable thickness evaporative cooling pads coupled to the condenser. Applied Thermal Engineering, 105: 1041-1050. https://doi.org/10.1016/j.applthermaleng.2016.01.067

[6] Chan, K.T., Yu, F.W. (2002). Applying condensing-temperature control in air-cooled reciprocating water chillers for energy efficiency. Applied Energy, 72(3-4): 565-581. https://doi.org/10.1016/S0306-2619(02)00053-3

[7] Roshani, A.S., Assareh, E., Ershadi, A. (2024). Optimization of a hybrid renewable energy system for off-grid communities. Renewable Energy, 236: 121425. https://doi.org/10.1016/j.renene.2024.121425

[8] Islam, M.S., Das, B.K., Das, P., Rahaman, M.H. (2021). Techno-economic optimization of a zero emission energy system for a coastal community in Newfoundland, Canada. Energy, 220: 119709. https://doi.org/10.1016/j.energy.2020.119709

[9] Li, Y., Sun, Y., Liu, J., Liu, C., Zhang, F. (2023). A data driven robust optimization model for scheduling near-zero carbon emission power plant considering the wind power output uncertainties and electricity-carbon market. Energy, 279: 128053. https://doi.org/10.1016/j.energy.2023.128053

[10] Harby, K., Al-Amri, F. (2019). An investigation on energy savings of a split air-conditioning system using different commercial cooling pad thicknesses and climatic conditions. Energy, 182: 321-336. https://doi.org/10.1016/j.energy.2019.06.031

[11] Harby, K., Gebaly, D.R., Koura, N.S., Hassan, M.S. (2016). Performance improvement of vapor compression cooling systems using evaporative condenser: An overview. Renewable and Sustainable Energy Reviews, 58: 347-360. https://doi.org/10.1016/j.rser.2015.12.313

[12] Hosoz, M., Kilicarslan, A. (2004). Performance evaluations of refrigeration systems with air-cooled, water-cooled and evaporative condensers. International Journal of Energy Research, 28: 683-696. https://doi.org/10.1002/er.990

[13] Islam, M.R., Jahangeer, K.A., Chua, K.J. (2015). Experimental and numerical study of an evaporatively-cooled condenser of air-conditioning systems. Energy, 87: 390-399. https://doi.org/10.1016/j.energy.2015.05.005

[14] Li, W., Shi, W., Wang, J., Lu, Y., Lu, J. (2021). Experimental study of a novel household exhaust air heat pump enhanced by indirect evaporative cooling. Energy & Buildings, 236: 110808. https://doi.org/10.1016/j.enbuild.2021.110808

[15] Chen, W.H., Mo, H.E., Teng, T.P. (2018). Performance improvement of a split air conditioner by using an energy saving device. Energy and Buildings, 174: 380-387. https://doi.org/10.1016/j.enbuild.2018.06.055

[16] Chua, K.J., Chou, S.K., Yang, W.M., Yan, J. (2013). Achieving better energy-efficient air conditioning - A review of technologies and strategies. Applied Energy, 104: 87-104. https://doi.org/10.1016/j.apenergy.2012.10.037

[17] Dhamneya, A.K., Rajput, S.P.S., Singh, A. (2018). Theoretical performance analysis of window air conditioner combined with evaporative cooling for better indoor thermal comfort and energy saving. Journal of Building Engineering, 17: 52-64. https://doi.org/10.1016/j.jobe.2018.01.012

[18] Faegh, M., Shafii, M.B. (2020). Thermal performance assessment of an evaporative condenser-based combined heat pump and humidification-dehumidification desalination system. Desalination, 496: 114733. https://doi.org/10.1016/j.desal.2020.114733

[19] Hajidavalloo, E. (2007). Application of evaporative cooling on the condenser of window-air-conditioner. Applied Thermal Engineering, 27(11-12): 1937-1943. https://doi.org/10.1016/j.applthermaleng.2006.12.014

[20] Hajidavalloo, E., Eghtedari, H. (2010). Performance improvement of air-cooled refrigeration system by using evaporatively cooled air condenser. International Journal of Refrigeration, 33(5): 982-988. https://doi.org/10.1016/j.ijrefrig.2010.02.001

[21] Teke, A., Timur, O. (2014). Assessing the energy efficiency improvement potentials of HVAC systems considering economic and environmental aspects at the hospitals. Renewable and Sustainable Energy Reviews, 33: 224-235. https://doi.org/10.1016/j.rser.2014.02.002

[22] Wang, T., Sheng, C., Nnanna, A.A. (2014). Experimental investigation of air conditioning system using evaporative cooling condenser. Energy and Buildings, 81: 435-443. https://doi.org/10.1016/j.enbuild.2014.06.047

[23] Yu, F.W., Chan, K.T. (2005). Application of direct evaporative coolers for improving the energy efficiency of air-cooled chillers. Journal of Solar Energy Engineering, 127(3): 430-439. https://doi.org/10.1115/1.1866144

[24] Manske, K.A., Reindl, D.T., Klein, S.A. (2001). Evaporative condenser control in industrial refrigeration systems. International Journal of Refrigeration, 24(7): 676-691. https://doi.org/10.1016/S0140-7007(00)00084-0

[25] Omara, Z.M., Abdullah, A.S., Dakrory, T. (2017). Improving the productivity of solar still by using water

fan and wind turbine. Solar Energy, 147: 181-188. https://doi.org/10.1016/j.solener.2017.03.041
[26] Pan, S., Pei, F., Wang, H., Liu, J., Wei, Y., Zhang, X., Li, G., Gu, Y. (2018). Design and experimental study of a novel air conditioning system using an evaporative condenser at a subway station in Beijing, China. Sustainable Cities and Society, 43: 550-562. https://doi.org/10.1016/j.scs.2018.09.013
[27] Ghanegaonkar, P.M., Jadhav, G.K., Garg, S. (2018). Performance improvement of turbo ventilators with internal blades. Advances in Building Energy Research, 12(2): 164-177. https://doi.org/10.1080/17512549.2016.1257439